academicJournals

Vol. 8(18), pp. 876-884, 16 May, 2013
DOI: 10.5897/IJPS12.578
ISSN 1992-1950 © 2013 Academic Journals
http://www.academicjournals.org/IJPS

International Journal of Physical Sciences

Full Length Research Paper

Performance evaluation of broadband access network based on subcarrier multiplexing (SCM): Spectral amplitude coding optical code division multiple access

Junita Mohd Nordin[1]*, Syed Alwee Aljunid[1], Anuar Mat Safar[1], Amir Razif Arief[1], Rosemizi Abd Rahim[1], R. Badlishah Ahmad[1] and Naufal Saad[2]

[1]School of Computer and Communication Engineering, University Malaysia Perlis, 01000 Perlis, Malaysia.
[2]School of Electric and Electronic Engineering, Universiti Teknologi Petronas, Tronoh, Perak, Malaysia.

Accepted 8 March, 2013

A hybrid spectrally amplitude coded (SAC) optical code division multiple access (CDMA) with subcarrier multiplexing (SCM) scheme is a potential candidate for future broadband access solutions in the communication network. In this work, the performance of hybrid technique is investigated. Theoretical derivations are developed based on the zero cross correlation (ZCC) code. The performances are evaluated taking into account the relevant noises such as thermal noise, shot noise and inter modulation noise. Design parameters such as number of optical channels, number of subcarriers, and input power are varied to see their effect on the system performances. Simulation analysis using Optisys simulator is also done and compared to the numerical theoretical results. We measured the performance based on the merits of received power, input power and bit error rates of the received signals. Results revealed that power penalty due to increased number of channels in the hybrid system is lower compared to the conventional OCDMA system, and hence improving the system performance in term of power efficiency. This exhibits the ability of the hybrid system to be one powerful technique as a candidate for future access network.

Key words: Spectral amplitude coding-optical code division multiple access (SAC-OCDMA), subcarrier multiplexing (SCM), zero cross correlation (ZCC), broadband access network.

INTRODUCTION

Recent years have seen the rapid growth of bandwidth hungry broadband access network which keeps the network and service providers busy finding ways of connecting the network up to the last mile solutions. Although fiber optics may seem to be the best option in the near future because of its huge amount of available bandwidth, the main issue of cost-constraint and the fact that it cannot eventually go everywhere makes the standalone access solution unreliable. On the other hand, wireless access solutions, despite of having a congested bandwidth, can eventually go everywhere with cheaper cost preferable by most end users. Moreover, the overwhelming advance of high speed electronics components makes the RF domain architecture still an ongoing technology. Thus, an ultimate solution that can satisfy the limitations in the broadband access network is the convergence of the optical access and wireless access to exploit the advantages of both architectures rather than their stand-alone architecture. This hybrid technology gives rise to the fiber-wireless (Fi-Wi) access networks, or also known as the Radio over Fiber (RoF) technology. Until date, there are quite a number of

*Corresponding author. E-mail: junita.unimap@gmail.com. Tel: +6094484494.

published works done on the Fi Wi networks architecture, mostly proposing on the Wavelength Division Multiplexing (WDM) architecture on the optical side (Ghazisaidi and Maier, 2009; Opatic, 2009). In this article, on the other hand, we proposed the application of optical code division multiple access (OCDMA) scheme instead of the WDM to be integrated with the RF domain in subcarrier multiplexing (SCM) manner.

Optical CDMA is getting more attention because of its ability to support asynchronous burst communications with higher level of security. It was employed initially for local-area (Smith et al., 1998), for access network applications (Pearce and Aazhang, 1994; Zhang et al., 1999) and also for emerging networks such as the generalized multiprotocol label switching (Maric et al., 1993). However, OCDMA system networks are limited by the multiple access interference (MAI), which occurs especially when large numbers of users are involved. Thus, in multi-service environments, the transmission capacity and the number of users can be increased by using the SCM technology that enables multiple RF signals to be transmitted simultaneously over the fiber-optic links (Kim et al., 2010). The SCM is an attractive technique where it provides the independency of different channels. This allows for great flexibility in the choice of modulation schemes. With this technique, the information signals are modulated onto different electrical subcarriers in the radio or microwave domain and combined together to modulate the intensity of an optical carrier. At the receiving part, a photo detector will convert the optical signal into an electric current. To retrieve the original signal, the electric current will then be demultiplexed and demodulated using a conventional method. One significant benefit of SCM is that the electrical components and equipments are far less expensive than its optical counterparts. Considering this advantage, we integrated the SCM into the OCDMA access network to investigate the effect on the system's performance. Related work on the area of hybrid SCM OCDMA has been done by Sahbudin et al. (2009, 2010) where the authors evaluated the performance of this hybrid technique based on different detection techniques. From their results, it is shown that the best performance of the hybrid system is by using the direct detection technique. On another related work by Abd et al. (2012), they concluded that the hybrid system can be improved in term of cardinality by selecting an appropriate code in OCDMA. In their study, the researchers utilized the multi diagonal (MD) code which has a zero cross correlation property compared to other codes evaluated in the research. Hence, in our work, we did not compare the results based on number of users or subcarriers since the zero cross correlation (ZCC) code used in this study also have the same property as in MD code. The originality in this paper lies in the evaluation on how increasing the channels in optical domain and subcarrier domain affect the power loss of the hybrid system.

MATERIALS AND METHODS

Hybrid SCM-OCDMA system description

The proposed hybrid OCDMA SCM system configuration is shown in Figure 1. The main difference between the hybrid architecture compared to the conventional OCDMA architecture lies in the added microwave domain in the transmitter and receiver part to represent the SCM architecture. At the transmitter, data with independent unipolar digital signal is mixed with a different microwave carrier (f_i), called the subcarriers. The subcarriers are then combined and optically modulated onto the code words (c_i) using an optical electrical modulator (OEM). In this paper, we utilized the ZCC code (Anuar et al., 2006) in the SAC- OCDMA code family because of its special feature where the cross correlation is always zero. The code structure does not have an overlapping of bit '1' and it will not cause the ZCC code to interfere between users. Eventually, this will definitely suppress the phase intensity induced noise (PIIN). Thus, only shot noise and thermal noise have been considered, ignoring PIIN due to zero cross-correlation between users.

The code words which are based on the ZCC code are generated with different wavelengths provided by the light source. Table 1 shows an example of ZCC code with weight two and three code words, where *λ1-λ6* represents the assigned wavelengths for each code. From Table 1, the assigned code words will be:

$$\text{Codeword}\begin{cases} optical\ channel\ 1 \ => \lambda_1\ \ \lambda_3 \\ optical\ channel\ 2\ => \lambda_2\ \lambda_5 \\ optical\ channel\ 3\ => \lambda_4\ \ \lambda_6 \end{cases}$$

The encoders consist of a multiplexer which will combine the different wavelengths to generate different code words. The *n* modulated code words are multiplexed together via a combiner and transmitted through the single mode fiber. Upon this stage, we can observe that each channel is actually assigned a subcarrier frequency, f_i, and a particular code word, c_i, where each pair ($f_{i,}$ c_i) is unique with respect to every other channel. Each channel of ($f_{i,}$ c_i) is representing one user in the system. At the receiver, the different modulated code words are separated by an optical decoder consisting of a splitter and multiplexers based on their assigned wavelengths. Then, the decoded signal is detected by the photo detector. A splitter and an electrical band pass filters are used to split the subcarrier multiplexed signals and reject unwanted signals, respectively. In order to recover the original transmitted data, the incoming signal is electrically mixed with a microwave frequency f_i and filtered using a low pass filter (LPF). In the transceiver scheme, it is important for the receiver to decode the correct code sequence and to be tuned to the correct RF frequency to ensure the receiver recovers the desired data signal while rejecting other unwanted signals. Therefore, this enables the hybrid scheme to support high transmission rate with a high level of security. The hybrid system design is based on the direct detection technique. The advantage of direct detection technique is that only one decoder and one detector are needed for each code sequence. This is achievable due to the zero cross correlation properties of the ZCC code where the information can be adequately recovered from any of the chips that do not overlap with any other chips from other code sequences. Accordingly, only the clean chips are filtered out by the decoder and detected by the photo detector.

System performance analysis

In the analysis of this hybrid SCM/OCDMA system, we have considered the effect of shot noise, thermal noise and also the inter-modulation distortion of subcarrier channels on the photo detector. The PIIN is ignored due to the zero cross correlation

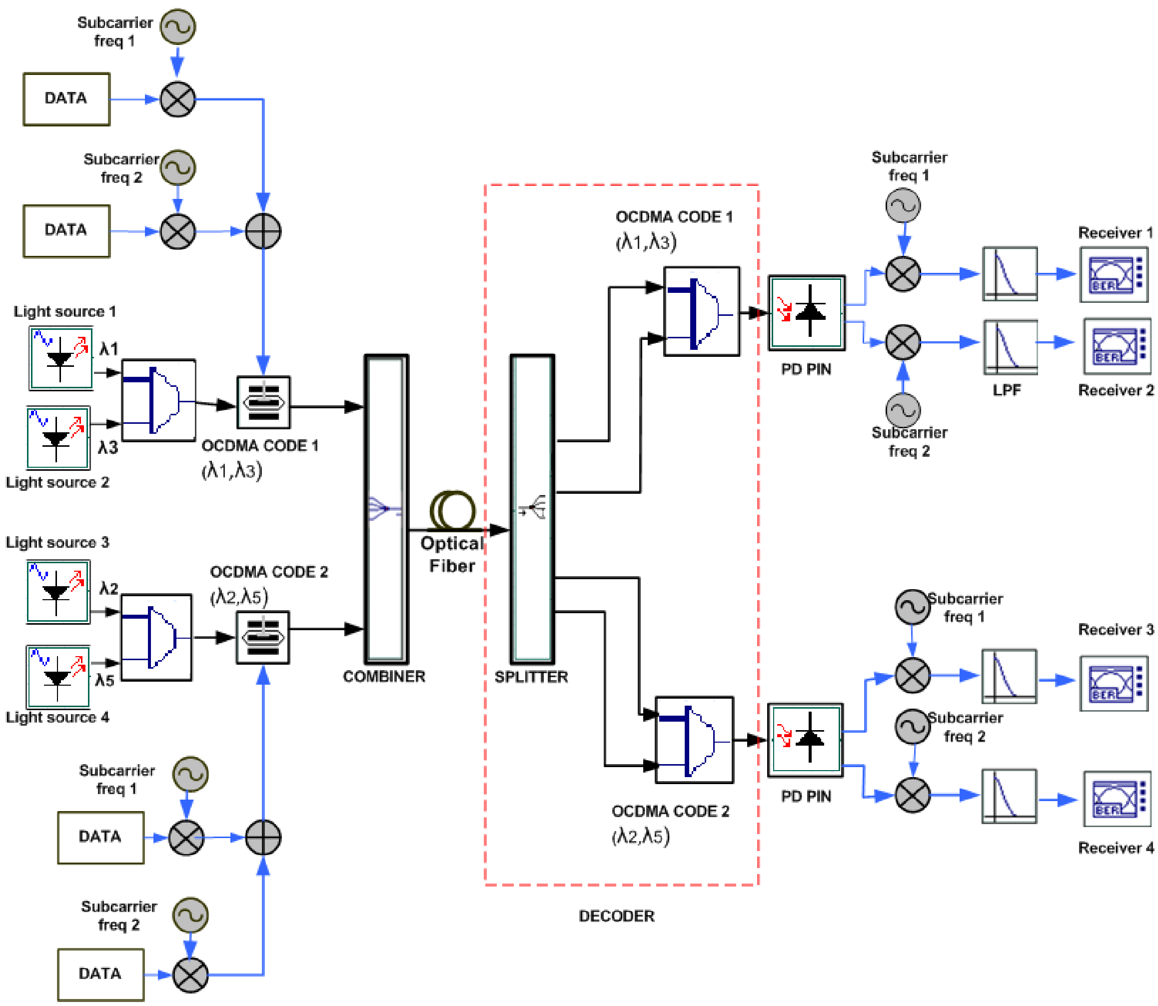

Figure 1. The hybrid SCM/OCDMA system configuration.

condition and no overlapping of spectra from different users. In our analysis, the following assumptions are made (Wei et al., 2001):

(i) Each light source spectra is ideally unpolarized and its spectrum is flat over the bandwidth $[v - \Delta v/2, v_0 + \Delta v/2]$ where v_0 is the optical center frequency and Δv is the optical source bandwidth in Hertz,
(ii) Each power spectral component has identical spectral width,
(iii) Each user has equal power at the receiver,
(iv) Each bit stream from each user is synchronized.

These assumptions are important for mathematical simplicity. Without these assumptions, it is difficult to analyze the system. To simplify our analysis, Gaussian approximation is used for all. The Gaussian's approximation is used in the calculation of bit error rate (BER) because the noises and disturbances that are always present in the communication systems are modeled quite accurately (Kazovsky et al., 1996; Lin et al., 2005). PIN photo detectors are used, and the dark current is assumed to be negligible. The spacing of optical carriers is assumed to be sufficiently wide so that the effect of crosstalk from adjacent channels is negligible (Chao, 1993). The subcarrier channels are equally spaced. Thus, the noise variances at the photo detector due to detection can be denoted as:

$$\left\langle i^2 \right\rangle = \left\langle I_{shot}^2 \right\rangle + \left\langle I_{thermal}^2 \right\rangle + \left\langle I_{IMD}^2 \right\rangle \tag{1}$$

where I_{shot} denotes the shot noise, $I_{thermal}$ is the thermal noise and I_{IMD} is the inter-modulation distortion noise due to the subcarrier channels. When incoherent light fields are mixed and incident upon a photo detector, the phase noise of the fields causes an intensity noise in term of photo detector output, where the source coherence time is expressed as (Smith et al., 1998):

$$\tau_c = \frac{\int_0^\infty G^2(v)dv}{\left[\int_0^\infty G(v)dv\right]^2} \tag{2}$$

where G (v) is the power spectral density (PSD) of the thermal source. Let $C_{k(i)}$ denotes the ith element of the kth ZCC code sequence, and the code properties for direct detection technique can be written as:

Table 1. ZCC code with weight two and three code words.

Code words	λ1	λ2	λ3	λ4	λ5	λ6
1st code word	1	0	1	0	0	0
2nd code word	0	1	0	0	1	0
3rd code word	0	0	0	1	0	1

$$\sum_{i=1}^{N} C_k(i)C_l(i) = \begin{cases} W \ for k = l \\ 0 \ \ for \ else \end{cases} \tag{3}$$

The power spectral density (PSD) of the received signal is Yang (2004):

$$r(v) = \frac{P_{sr}}{\Delta v}\sum_{k=1}^{K} d_k(t)\sum_{i=1}^{L} C_k(i)C_l(i)rect(i) \tag{4}$$

K represents the number of ZCC code sequences, where each carrying their own subcarrier channels; L is the ZCC code length; P_{sr} is the effective power of broadband source at receiver, with bandwidth =Δv; $d_{k(t)}$ is the modulated data of the nth subcarrier on the kth optical code; which can be denoted as:

$$d_k(t) = \sum_{n=1}^{Nc} u_{n,k}(t) m_{n,k} \cos(\omega_n t) \tag{5}$$

$u_{n,k(t)}$ denotes the normalized digital signal of “0” and “1” at the nth subcarrier channel of the kth code, while $m_{n,k}$ is the modulation index of the nth subcarrier of the kth code. N_c is the number of subcarrier channels in each code sequence and ω_n is the angular subcarrier frequency. Here, we assume that the modulation index is identical for all subcarrier channels (Hui et al., 2002), thus,

$$0 < m_{n,k} \leq \frac{1}{N_c}; \tag{6}$$

The *rect (i)* function in Equation (4) is denoted as:

$$rect(i) = u\left[v - v_0 - \frac{\Delta V}{2L}(-L+2i-2)\right] - u\left[v - v_0 - \frac{\Delta V}{2L}(-L+2i)\right] = \left\{u\left[\frac{\Delta V}{L}\right]\right\} \tag{7}$$

where $u(v)$ is the unit step function. The PSD at the input of the photo detector at the lth receiver during one data bit period can be expressed as $G_{dd}(v)$, which equals to $r(v)$ as stated in Equation (4). Hence, the total power incident at the input of the photo detector is written as:

$$\int_0^{\infty} G_{dd}(v)dv = \int_0^{\infty}\left[\frac{P_{sr}}{\Delta v}\sum_{k=1}^{K} d_k(t)\sum_{i=1}^{L} C_k(i)C_l(i)\left\{u\left[\frac{\Delta v}{L}\right]\right\}\right]dv \tag{8}$$

$$= \frac{P_{sr}}{\Delta v}\cdot\frac{\Delta v}{L}\sum_{k=1}^{K} d_k(t)\sum_{i=1}^{L} C_k(i)C_l(i) \tag{9}$$

Thus,

$$\int_0^{\infty} G_{dd}(v)dv = \frac{P_{sr}}{L} W d_l \tag{10}$$

The desired signal for a particular user is obtained by expressing the photocurrent, I as:

$$I = I_{dd} = \Re\int_0^{\infty} G_{dd}(v)dv \tag{11}$$

where $\Re$ is the responsivity of the photodetector denoted as:

$$\Re = \frac{\eta e}{h v_c} \tag{12}$$

η is the quantum efficiency, e is the electron’s charge, h is the Planck’s constant, and v_c is the central frequency of the original broadband pulse. Substituting Equation (10) into the Equation (11) we obtain

$$I = \Re\left[\frac{P_{sr}}{L} W d_l\right] \tag{13}$$

Substituting Equation (5) into Equation (13), the desired photocurrent signal for the kth channel can be written as:

$$I = \Re\frac{P_{sr}}{L} W \sum_{n=1}^{Nc} u_{n,k}(t) m_{n,k} \cos(\omega_n t) \tag{14}$$

The desired signal is then driven to the RF demodulator and mix coherently with a local oscillator given by 2cos (ω_nt). The signal becomes

$$I = \Re\frac{P_{sr}}{L} W \sum_{n=1}^{Nc} u_{n,k}(t) m_{n,k} \cos(\omega_n t)[2\cos(\omega_n t)] \tag{15}$$
$$= \Re\frac{P_{sr}}{L} W \sum_{n=1}^{Nc} u_{n,k}(t) m_{n,k}\left[2\cos^2(\omega_n t)\right]$$

Simplified by using trigonometric identities, I is expressed as

$$I = \Re\frac{P_{sr}}{L} W \sum_{n=1}^{Nc} u_{n.k}(t) m_{n,k}[1+\cos(2\omega_n t)] \tag{16}$$

At the receiver’s end, the doubled frequency component is filtered out using low pass filter (LPF). Thus the output of the RF demodulator can be expressed as:

$$I = \frac{\Re P_{sr} W}{L} u_{n,k}(t) m_{n,k} \tag{17}$$

$u_{n,k}(t)$ is the normalized digital ≈ 1. For the noise variances, we only consider shot noise, thermal noise and inter-modulation distortion

Table 2. The parameters used for BER calculation.

Symbol	Parameter	Value
η	Photodetector quantum efficiency	0.6
Δv	Linewidth broadband source	3.75THz
λ_0	Operating wavelength	1550nm
B	Electrical bandwidth	80MHz/311MHz
R_b	Data bit rate	155Mbps/622Mbps
T_n	Receiver noise temperature	300K
R_L	Receiver load resistor	1030Ω
E	Electron charge	1.6x10^{-19}C
H	Planck's constant	6.66 x10^{-34} Js
K_b	Boltzmann's constant	1.38 10^{-23}J/K

(IMD) noise. The noise power for shot noise is given as:

$$\left\langle I_{shot}^2 \right\rangle = 2eBI_{dd} \tag{18}$$

Substituting I_{dd} in Equation (18), assuming all users transmitting bit "1", we get

$$\left\langle I_{shot}^2 \right\rangle = 2eB\frac{\Re P_{sr} W}{L} \tag{19}$$

The thermal noise is given by Papannareddy (1997);

$$\left\langle I_{thermal}^2 \right\rangle = \frac{4K_B T_N B}{R_L} \tag{20}$$

where $K_b, T_n, B, \text{and } R_L$ is the Boltzmann constant, absolute receiver noise temperature, noise equivalent electrical bandwidth of the receiver and receiver load resistor respectively. The inter-modulation distortion noise as expressed in Koshy and Shankar (1997, 1999) is:

$$\left\langle I_{IMD}^2 \right\rangle = P_{sr}^2 \Re^2 m_{n,k}^6 \left[\frac{D_{111}}{32} + \frac{D_{21}}{64}\right] \tag{21}$$

where D_{111} is the three tone third order inter-modulation at $f_i + f_k - f_l$; given by

$$D_{111} = \frac{r}{2}(N - r + 1) + \frac{1}{4}\left[(N-3)^2 - 5\right] - \frac{1}{8}\left[1 - (-1)^N\right](-1)^{N+r} \tag{22}$$

where N is the number of subcarrier channels which in this case is equal to N_c, r is the rth subcarrier. D_{21} is the two tone third order modulation at $2f_i - f_k$; given by

$$D_{21} = \frac{1}{2}\left[N - 2 - \frac{1}{2}\left\{1 - (-1)^N\right\}(-1)^r\right] \tag{23}$$

The total noise here can then be expressed as

$$\left\langle i^2 \right\rangle = \left\langle I_{shot}^2 \right\rangle + \left\langle I_{thermal}^2 \right\rangle + \left\langle I_{IMD}^2 \right\rangle$$

$$\left\langle i^2 \right\rangle = 2eB\frac{\Re P_{sr} W}{L} + \frac{4K_B T_N B}{R_L} + P_{sr}^2 \Re^2 m_{n,k}^6 \left[\frac{D_{111}}{32} + \frac{D_{21}}{64}\right]$$

The SNR of the hybrid SCM/OCDMA using ZCC code can be written as

$$SNR = \frac{(I)^2}{\left\langle i^2 \right\rangle}$$

$$SNR = \frac{(I)^2}{\left\langle i^2 \right\rangle} = \frac{\frac{\Re^2 P_{SR}^2 W^2}{L^2} m_{n,k}^2}{\frac{2eBP_{SR}W}{L} + \frac{4K_B T_n B}{R_L} + P_{SR}^2 \Re^2 m_{n,k}^6 \left[\frac{D_{111}}{32} + \frac{D_{21}}{64}\right]} \tag{24}$$

The BER can be obtained from the SNR by employing Gaussian approximation:

$$BER = 0.5 * erfc\left(\sqrt{\frac{SNR}{8}}\right) \tag{25}$$

Where the error function erfc (x) can be defined as Larry (1998);

$$erfc(x) = \frac{2}{\sqrt{\pi}} \int_0^x e^{-t^2} dt \tag{26}$$

Typical error rates for optical fiber telecommunication systems is 10^{-9}. This error rate depends on signal to noise ratio at the receiver. The typical parameters used for BER calculation in this study are summarized in Table 2.

Network simulation setup

The hybrid system has been simulated using the software "*Optisys*" Version 6.0. We vary the design parameters such as the number of OCDMA channels and number of subcarrier channels to observe their effect in the simulated environment. The optical channel chip width is equal to 0.8 nm while the subcarrier frequency spacing is

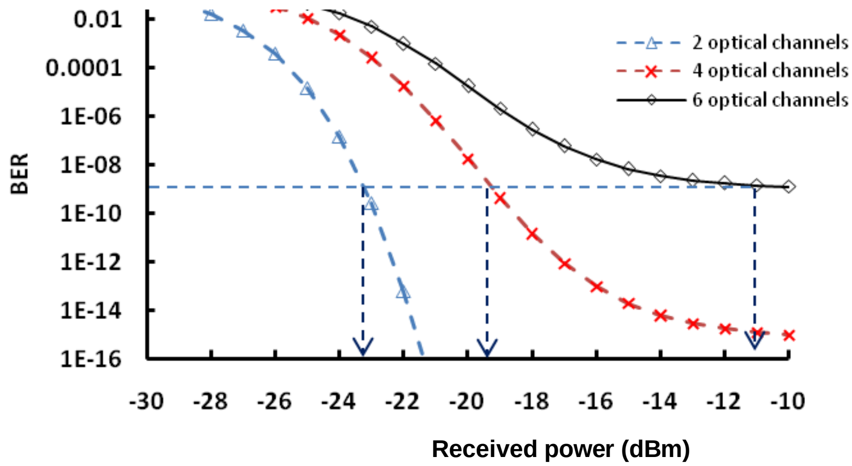

Figure 2. Bit error rates (BER) versus received power for the conventional OCDMA network when optical channels are increased from 2, 4 and 6.

set to 600 MHz. In addition, to avoid clipping in the data spectrum, the subcarrier frequencies are set to be equal or larger than twice the bit rate assigned. The transmission medium used in the simulation is the standard single mode fiber (ITU-T G.652). To set the simulation as close to the real environment as possible, the nonlinear effects such as the four wave mixing and self-phase modulation are activated according to their typical industrial values. Accordingly, attenuation and dispersion effects are set to be at 0.25 dB/km and 18 ps/nm-km. For the receiver, we set the photo detector thermal noise coefficient at 1.8×10^{-23} W/Hz, while the dark current value is set to be 5nA. BER analyzers are placed at the end of the receiver's output to evaluate the bit error rates and observe the eye pattern of each received signal.

RESULTS AND DISCUSSION

To ensure that the fiber system has sufficient power for correct operation, network designer needs to calculate the span's power budget, which is the maximum amount of power it can transmit. From a design perspective, worst-case analysis calls for assuming minimum transmitter power and minimum receiver sensitivity. This provides for a margin that compensates for variations of transmitter power and receiver sensitivity level. Our objective is to investigate how an increasing number of channels affect the power penalty loss of the system. We then compare the conventional all optical OCDMA with a system with hybrid SCM OCDMA. Figure 2 shows the variation of BER over received power in the conventional OCDMA system as the number of channels is increased. Here, each code word represents one channel (that is, one user or subscriber).

To increase the number of channels, we need to increase the number of code words. We can see that the BER degrades as the received power gets smaller. It must be noted that even a very small fall in optical signal power can deteriorate the BER by some order of magnitudes. It is obvious in Figure 2, at the 10^{-9} BER, the received power at photo detector is -23 dBm for 2 optical channels and -19 dbm for 4 optical channels. The error flooring at BER of 10^{-9} occurs at -11 dBm received power for 6 optical channels. Thus the power penalty loss here is about 12dB when we increase the channels from two to six in the all-optical environments. Clearly, even a small increase in the number of optical channels, the required receiver sensitivity power increased significantly. This leads to a huge difference in the amount of power that needs to be transmitted at the transmitter side. It is also evident that the BER degrades with the increase number of channels because, as channels are increased, the code length of the system will also increase. The larger the code lengths (L), means a larger bandwidth is needed for the system. Noise power is proportional to bandwidth. Larger bandwidth will cause a higher noise power level, thus, lowering the signal –to noise ratio of the system. Hence, BER will degrade. This can be described by SNR and BER equation in the article in Equation (24) and (25). In addition, as the number of channels increase, the MAI from other users will be a limiting factor, and hence, results in degrading the BER.

Figure 3, on the other hand shows the relation of BER and received power with a fixed optical channel (fixed code word) and increase number of subcarrier channels. The received power sensitivity is shown to be increased in smaller range values when the subcarriers are increased from three to six subcarriers. For BER of 10^{-9} error floor, a system with three subcarriers shows a -23dBm receiver sensitivity, while the system with four and six subcarriers only needs an increased receiver sensitivity of -22dBm and -20dBm. Here, the power penalty loss with increased channels from three to six is only about 3dB. This difference ranges is much smaller as compared to increasing the number of optical channels.

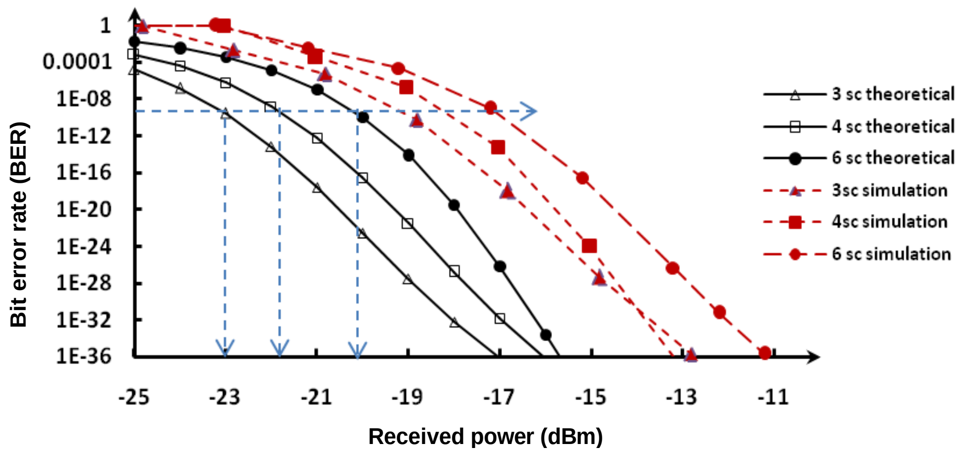

Figure 3. BER against received power with different number of subcarriers for theoretical (black lines) and simulations (red dashes).

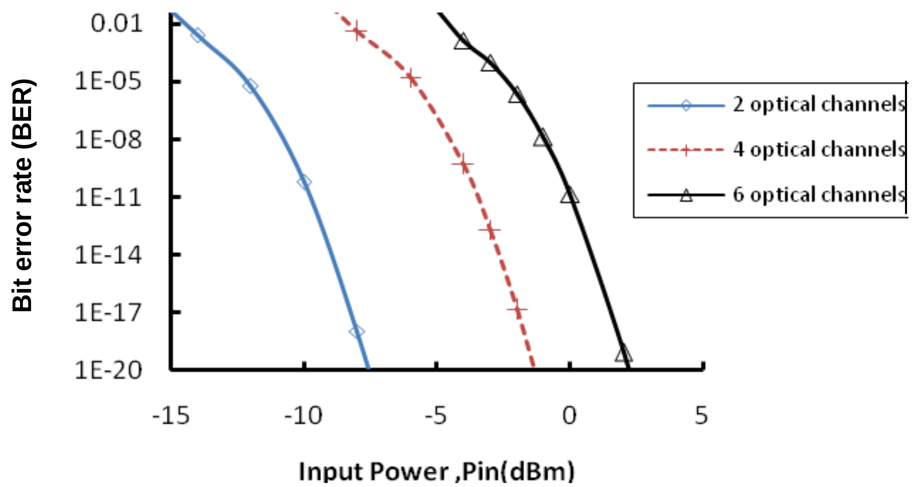

Figure 4. BER against input power simulated with various numbers of optical channels.

Figure 3 also includes the simulation result using Optisys software of a system with fixed optical channel equals to two (two OCDMA codes) and subcarriers channels equal to three, four and six. The BER curves of the simulation parts are plotted in red dashes. As expected, the plot of BER over received power curves of the simulation shows relatively the same patterns as compared to the theoretical curves in black lines. In addition, BER is depicted to be deteriorating when the number of sub channels is increased. In SCM OCDMA system, as the number of sub channels is increased, inter-modulation distortion products of the second and third order harmonics will also increase. Thus, this will degrade the BER as these harmonics can combine or overlap with the original signal and destructively decrease or reduce the signal power of the original signal. Again, the SNR decrease, and finally the BER are deteriorated.

Figures 4 and 5 indicate the simulation result to validate our previous discussion by showing the variations of BER dependences over input power. In Figure 4, to achieve a BER of 10^{-9}, the required input power for two optical channels is -10dBm. As the optical channels are increased to four and six, input power required also increased to -4dBm and 0dBm, respectively. A total power loss of 10dB in the transmitted power is observed when we increase the number of channels from two to six. In contrast, when subcarrier channels in Figure 5 are increased from three to four and finally to six sub channels, the input powers required by the system are from -10 dBm to about -8 dBm, which is only about 2 dB power penalty lost. This is a significant difference in the power range from that in Figure 4. Thus, it is clearly demonstrated that to accommodate a larger number of subscribers, power consumptions are

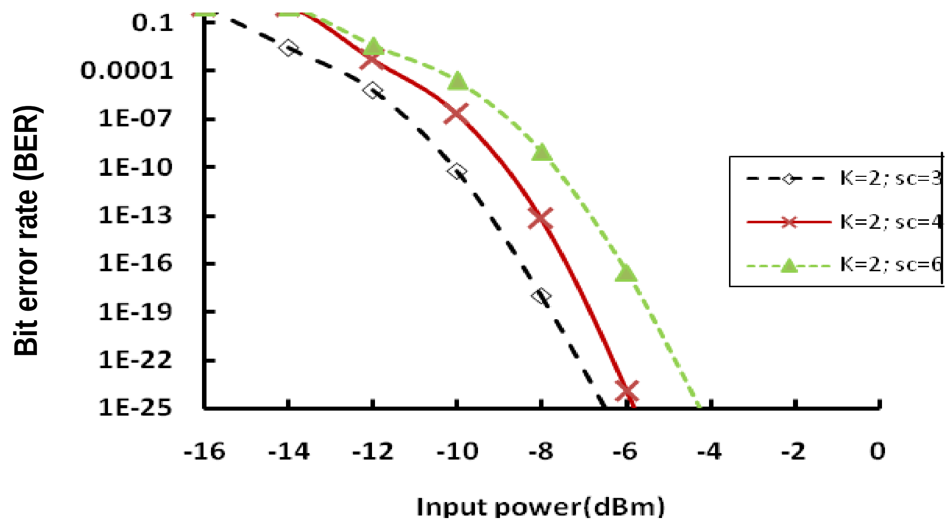

Figure 5. BER against input power simulated with different number of subcarrier channels.

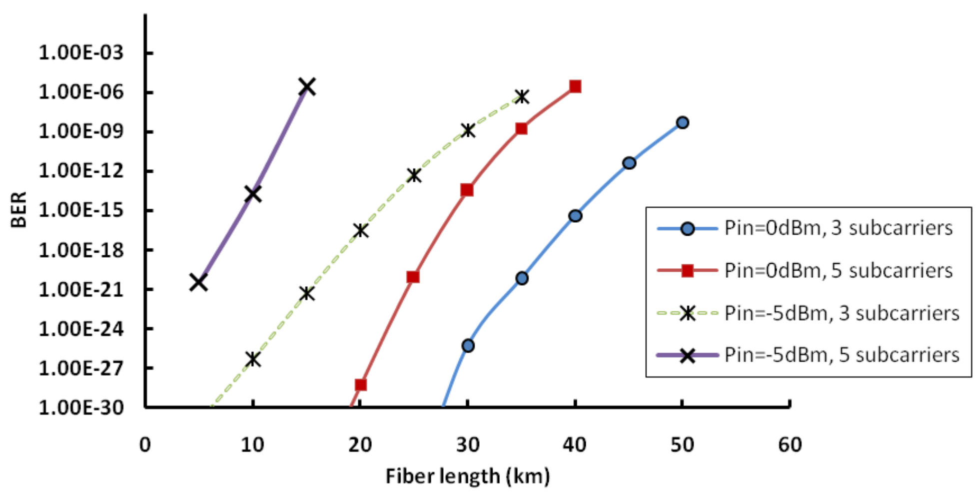

Figure 6. Variation of BER with respect to fiber length for different subcarrier numbers.

improved in a hybrid system compared to the conventional system.

Figure 6 depicts the variation of BER with respect to fiber length for three and five subcarriers when different input powers are fed to the system. It is observed that the BER degrades as the transmission distance increases. The dispersion and attenuation increases as the optical fiber length increases, thus decreasing the BER. The curves show that the system can perform well with an acceptable BER better than 10^{-9} for up to 50 km for the system occupying three subcarriers with input power of 0dBm and 35 km for five subcarriers. It is obvious that larger number of subcarrier channels will degrade the system performance. In addition, lower input power will result in shorter achievable distance for the acceptable BER of 10^{-9}.The system with three subcarriers can be transmitted up to 30 km with -5dBm input power, while for five subcarriers channel can only be transmitted up to 15 km.

Conclusion

This work presents an analytical and simulated performance of a hybrid subcarrier multiplexing over optical CDMA based on ZCC code. Our work reveals that system performance in term of power penalty loss is improved via the proposed hybrid SCM OCDMA system based on the observation of BER curves over transmitted and received power. In addition, it is apparent that the theoretical and simulation both have almost similar relation patterns and results in the hybrid performances. We have ascertained that to achieve large cardinality broadband access network, this hybrid system is a more preferable architecture compared to conventional all optical OCDMA. This work can be a future guide to more intensive research on hybrid network. The SCM/OCDMA system could be one promising solution to the symmetric high capacity network with high spectral efficiency, cost effective, good flexibility and enhanced security, an attractive candidate for next generation broadband access networks.

REFERENCES

Abd TH, Aljunid SA, Fadhil HA, Radhi IF, Ahmad RB, Rashid MA (2012). Performance improvement of hybrid SCM SAC-OCDMA networks using multi-diagonal code. Sci. Res. Essays 7(11):1262-1272.

Anuar MS, Aljunid SA, Saad NM (2006). Development of a New Code for Spectral-Amplitude Coding Optical Code Division Multiple Access (OCDMA). IJCSNS Int. J. Comput. Sci. Netw. Secur. 6:180-184.

Chao L (1993). Effect of laser diode characteristics on the performance of an SCM OFDM direct detection system. IEE Proc. J. Optoelectron. 140:392-396.

Ghazisaidi N, Maier M (2009). Fiber-Wireless (FiWi) Access Networks:A Survey. IEEE Commun. Mag. pp. 160-167.

Hui R, Zhu B, Huang R, Allen CT, Demarest KR, Richards D (2002). Subcarrier Multiplexing for High Speed Optical Transmission. J. Lightwave Technol. 20:417-427.

Kazovsky L, Benedetto S, Willner A (1996). Optical Fiber Communication Systems. Artech House, Inc.

Kim K, Jeoung J, Lee J (2010). Effect of Fiber Dispersion and Self Phase Modulation in Multi-channel Subcarrier Multiplexed Optical Signal Transmission. J. Opt. Soc. Korea 14:351-356.

Koshy BJ, Shankar PM (1997). Efficient Modeling and Evaluation of Fiber-fed Microcellular Networks in a Land Mobile Channel using a GMSK Modem Scheme. J. IEEE. Selected Areas Commun. 15:694-705.

Koshy BJ, Shankar PM (1999). Spread Spectrum techniques for fiber-fed microcellular networks. J. IEEE. Trans. Vehicul. Technol. 48:847-857.

Larry CA (1998). Special Functions of Mathematics for Engineers 2^{nd}. Ed. SPIE Press and Oxford University Press.

Lin CH, Wu J, Tsao HW, Yang CL (2005). Spectral amplitude-coding optical CDMA system using Mach–Zehnder interferometers. IEEE J. Lightwave Technol. 23:1543-1553.

Maric SV, Kostic ZI, Titlebaum EL (1993). A new family of optical code sequences for use in spread-spectrum fiber-optic local area networks. IEEE Trans. Commun. 41:1217-1221.

Opatic D (2009). Radio over Fiber Technology for Wireless Access. GSDC Croatia.

Papannareddy R (1997). Introduction to Lightwave Communication Systems. Artech House, Inc. P. 246.

Pearce MB, Aazhang B (1994). Multiuser detection for optical code division multiple access system. IEEE Trans. Commun. 42:1801-1810.

Sahbudin RKZ, Abdullah MK, Mokhtar M (2009). Performance improvement of hybrid subcarrier multiplexing optical spectrum code division multiplexing system using spectral direct decoding detection technique. Opt. Fiber Tech. 15:266-273.

Sahbudin RKZ, Abdullah MK, Mokhtar M, Anas SBA, Hitam S (2010). Performance of Subcarrier-OCDMA System with Complementary Subtraction Detection Technique. Int. J. Info. Commun. Eng. 6(4):248-253.

Smith EDJ, Blaikie RJ, Taylor DP (1998). Performance enhancement of spectral-amplitude-coding optical CDMA using pulse-position modulation. J. IEEE. Trans. Commun. 46(9):1176-1185.

Smith GH, Novak D, Lim C (1998). A millimeter-wave full-duplex WDM/SCM fiber-radio access network. OFC ’98, paper TuC5.

Wei Z, Shalaby HMH, Ghafouri-Shiraz H (2001). Modified quadratic congruence codes for fiber Bragg-grating-based spectral-amplitude-coding optical CDMA systems. J. Lightwave Technol. 19(9):1274-1281.

Yang CC, Huang JF, Tseng SP (2004). Optical CDMA Network Codecs Structured with M-Sequence Codes over Waveguide-Grating Routers. IEEE Photonics Technol. Let. 16:641-643.

Zhang X, Ji Y, Chen X (1999). Code routing technique in optical network. Beijing Univ. Posts Telecomm. 1:416-419.